X-662-75-152

PREPRINT

NASA TM X- 70923

# COSMIC RAY POSITRON AND NEGATRON SPECTRA BETWEEN

# MEASURED IN 1974



R. C. HARTMAN

C. J. PELLERIN


JUNE 1975

GODDARD SPACE FLIGHT CENTER

GREENBELT, MARYLAND

# COSMIC RAY POSITRON AND NEGATRON SPECTRA BETWEEN 20 AND 800 MEV MEASURED IN 1974

R.C. Hartman and C. J. Pellerin

NASA/Goddard Space Flight Center
Greenbelt, Maryland 20771

## ABSTRACT

A balloon-borne spark chamber magnetic spectrometer has been used to measure separate spectra of positrons and negatrons in two flights during Summer, 1974. The flights reached atmospheric depths of 1.9 and 1.5 g $cm^{-2}$ after slow ascents which enhance the statistical accuracy of the atmospheric secondary subtraction. The total electron flux is about 0.3 $m^{-2}$ $s^{-1}$ $sr^{-1}$ $MeV^{-1}$ between 70 and 800 MeV, and increases toward lower energies. The positron spectrum decreases sharply toward lower energies from a value of about 0.08 $m^{-2}$ $s^{-1}$ $sr^{-1}$ $MeV^{-1}$ at 650 MeV, and only upper limits are obtained for positrons below 200 MeV. The implications of these data are examined with regard to the problem of solar modulation. At energies above 180 MeV, the spherically symmetric Fokker-Planck equation with a diffusion coefficient proportional to particle rigidity provides reasonable fits to both the positron and total electron data. At energies below 180 MeV the data are consistent with a continuation of the same diffusion coefficient and local source of negatrons, or a change in the diffusion coefficient to a constant value.

## I. INTRODUCTION

Cosmic ray positrons and negatrons in the energy range from 15 to 800 MeV are of astrophysical interest because of their ability to probe solar modulation. This paper presents measurements of these particles made with a balloon-borne magnetic spectrometer. Precise measurements of these particles have, in the past, been hampered by several factors. The overwhelming background of cosmic-ray protons and the desirability of separation into $e^+$ and $e^-$ has required complex instrumentation. The interpretation of fluxes measured with balloon-borne instrumentation has required an accurate knowledge of the contribution due to secondary electron production in the atmosphere. This knowledge can be obtained by combining a measurement of positron and negatron fluxes as a function of atmospheric depth with an appropriate theoretical model.

The data presented in this paper represent a reasonable optimization of those parameters given the constraints of balloon experimentation. Very large balloons (30 million and 50 million cubic feet) provided float measurements under a minimum of residual atmosphere. Slow ascents were used to provide accurate experimental growth curves. These data were then analyzed using a recent theoretical analysis of atmospheric secondary electron production and propagation to extract the contribution to the measured fluxes from sources external to the earth.

## II. INSTRUMENT AND BALLOON FLIGHTS

The detector system used in these flights is very similar to that described by Daugherty (1974) and Daugherty, Hartman and Schmidt (1975). Therefore, only a brief summary is presented here, with more

detailed description of only those features which differ from the earlier version of the instrument.

The apparatus, which is shown in Figure 1, utilizes magnetic core digital spark chambers to determine the trajectories of charged particles through the instrument, before and after they pass the gap of a permanent magnet. The direction and magnitude of the magnetic deflection provides the sign and rigidity of each particle traversing the detector. The spark chambers are triggered by a counter telescope consisting of a directional gas Cerenkov counter and two plastic scintillation counters. In addition, two anti-coincidence scintillation counters are used to veto events in which a particle fails to pass through the magnet gap.

The Cerenkov counter contains Freon-12 at 1 atm. pressure, which provides an energy threshold of about 21 $mc^2$ for a particle of mass m. In principle, the gas Cerenkov counter is insensitive to all protons and heavier nuclei with rigidities in the range of interest here (<1 GV) as well as all upward moving particles within the telescope aperture. Occasionally, however, a noise pulse from one of the Cerenkov photomultiplier tubes may occur in coincidence with the passage of a low-energy or upward moving particle through the telescope. As these random coincidences can yield particle trajectories which mimic good events, the reliability of electron identification has been enhanced by the use of two plastic scintillation counters D1 and D2 at depths of $\sim$1 and 3 radiation lengths of lead. For rigidities below 450 MV they serve primarily as range counters for nuclei since, for example, a proton must have a rigidity of at least 350 MV to reach D1, and at least 440 MV to reach D2. In addition, a proton which reaches D1 but not D2 must pro-

duce a signal in D1 of at least 5X minimum ionizing, and a proton which penetrates both D1 and D2 produces signals in D1 and D2 which are predictable from the measured rigidity. The two coincidence counters S1 and S2 are also pulse height analyzed, and are important in eliminating nucleon background above about 200 MV. These data, along with the spark chamber data, are telemetered to the ground in a PCM format and recorded on magnetic tape.

The experiment was flown on two balloons launched from Fort Churchill, Manitoba, on July 15 and August 3, 1974. The flights were planned to provide accurate positron and negatron flux measurements not only at the balloon float altitudes, but also for all atmospheric depths less than about 100 g $cm^{-2}$. These ascent curves are essential for the estimation of primary and atmospheric secondary contributions to the observed fluxes.

Unusually slow balloon ascents(1-2.5m $sec^{-1}$) were used in both flights to enhance the statistical accuracy of the ascent curves. Primary electrons of low rigidity are observable from the Churchill area only between about 1800 CST and 0600 CST (Jokipii et al., 1968; Webber, 1968; Israel and Vest, 1969; Daugherty et al., 1975). To avoid effects of the change from return albedo electrons (daytime) to primary electrons (night time) each flight was launched during the early evening. This allowed the slow ascent to bring the balloon to float altitude well before the increase in geomagnetic cutoff around 0600. The actual launch times were approximately 1830 CST July 15 and 2030 CST August 3, with float altitudes being reached only after balloon sunrise, about 0400 CST for both flights. The time at float altitude before the geo-

magnetic cutoff change was only about two hours, which was less than the planned time, but nevertheless satisfactory.

The balloons reached float altitudes of 142,000 ft (1.9 g $cm^{-2}$) and 154,000 ft (1.5 g $cm^{-2}$). For rigidities greater than 200 MV (above the variable geomagnetic cutoff), 18 hours of float data were obtained for the two flights combined.

## III. DATA ANALYSIS

Processing and analysis of the data was in many respects similar to that described by Daugherty (1974) and Daugherty et al. (1975); only those procedures which have changed substantially will be detailed here.

The data for a single event consists of a variable-length list of set core (spark) addresses from the spark chamber, and the pulse-height data from the four scintillation counters. The spark chamber data were first processed by a pattern recognition computer program which classifies events as "good" (to be included in further processing), "bad" (deleted), or "undecided" (the program unable to make a decision). The events classified as "good" are required to show a single track traversing the instrument within the nominal aperture with no obvious deflections except as expected in the magnet gap region. Spurious set cores are ignored if they do not appear to form a second track. "Bad" events are those which, for instance, show either no complete tracks or more than one track through the instrument, or which appear to scatter from a pole face of the magnet. Approximately 95% of the 100,000 events recorded during the two flights were classified as either "good" or "bad" by the pattern recognition program. The remaining "undecided" events were examined using an interactive graphics unit where they could be deleted,

or edited and accepted, by the operator. Most of the events examined in this way were deleted because no complete track was discernible or because the track was obviously outside the instrument aperture. The fraction of the graphically edited events which were accepted (∿20%) showed evidence of short delta ray tracks or low spark efficiency in some region of the spark chamber. The events accepted graphically were tagged and merged with the original "good" events, which were then subjected to a least-squares fitting program to determine the particle trajectories. The rigidity of each particle was calculated from its magnetic deflection using a detailed map of the magnetic field, including the fringe fields. Each event was examined and tagged for anomalies such as missing one of the counters in the system or a deflection not fully compatible with that expected in the magnetic field.

The angular deflection zero-reference and resolution were obtained from a histogram of deflection angles for those events which showed approximately minimum ionization in all four analyzed counters. A correction of 2 milliradians was found to be necessary, and the deflection angle resolution was found to be about 2 milliradians FWHM. The highest rigidity used in this analysis (800 MV) produces an angular deflection of about 9 milliradians.

In order to eliminate possible background from protons or other cosmic-ray nuclei, restrictions were placed upon the pulse-heights in the four analyzed counters. Since the energy deposited by a nucleus in each scintillator is uniquely determined if the rigidity is known, the restrictions were initially formulated so that any events were assumed to result from electrons which did not conform to the pulse-heights

expected for a nucleus with a rigidity determined from the spark chamber analysis, with suitable allowance for both rigidity and pulse-height resolution. With these rather loose restrictions it was found that, for positrons with energies above 120 MeV, a significant background existed on S1 vs. S2 pulse-height plots, which was not present in the corresponding negatron plots. Additional restrictions have thereofre been included which require the pulse-heights in the coincidence scintillators to be less than some (energy dependent) maximum value. This reduces the electron recognition efficiency (determined from the negatrons) to about 88% above 120 MeV, compared with 97-99% at lower energies.

The event rates for electrons in various rigidity intervals were examined to find the time of the change of geomagnetic cutoff mentioned above. The change was apparent in all rigidity intervals below 200 MeV. The time of the change appears to be rigidity dependent, but is the same for positrons and negatrons in a given rigidity range. Positron and negatron fluxes were therefore combined as shown in Figure 2.for each flight. Although in both flights the cutoff change appears to occur substantially later at the higher rigidities, only the first two float intervals of each flight were used for rigidities below 200 MeV. The entire float period was used for rigidities above 200 MeV.

The observed positron and negatron fluxes contain both primary and atmospheric contributions. In order to estimate the primary components it is necessary to examine the fluxes as a function of atmospheric depth. We have fitted the measured fluxes to functions of the form

$$J(T,X) = a(T)\ p(T,X) + b(T)\ s(T,X)$$

where p and s are the primary and secondary fluxes as a function of

atmospheric depth (X) and energy (T). We have used for s(T,X) the calculation by Daniel and Stephens (1974) for zero cutoff rigidity and solar minimum conditions.

The function p(T,X) must be obtained iteratively. A primary spectrum $P_0(T,0)$ is assumed (actually, a variety of initial spectra were tried) and numerically propagated through the atmosphere using bremsstrahlung and ionization energy losses to obtain $P_0(T,X)$. This function is then used in a least squares fit to the equation, yielding the multiplier a(T) for each energy separately. The next estimate for the primary spectrum above the atmosphere is thus $P_1(T,0) = a(T)$ $P_0(T,X)$, which can again be propagated through the atmosphere to give $P_1(T,X)$. The $P_2(T,0)$ obtained from the third least-squares fit to the preceeding equation does not differ appreciably from $P_1(T,0)$ and is thus the best estimate of the primary flux at energy T. Ascent data for several representative rigidity intervals are shown in Figure 3, along with the fitted primary, secondary and total curves.

In some cases the procedure outlined above gives primary fluxes within one standard deviation of zero, some of which are negative (due to use of Gaussian statistics). In these cases, the iterative procedure has been redone using a Poisson analysis which prohibits negative flux values. The results from this calculation are 95% confidence upper limits for the desired fluxes.

## IV. RESULTS AND DISCUSSION

Figure 4 shows the positron and negatron spectra obtained from the analysis described above, and Figure 5 compares our total electron spectrum with those from other measurements near solar minimum.

The present fluxes fall substantially below those from the nearly identical experiment carried out in 1972 (Daugherty, 1974; Daugherty et al., 1975). This might be explained by the lower solar activity in 1972, as indicated by high-latitude neutron monitor levels about 2% higher than in 1974. However, low energy protons observed by the Pioneer spacecraft network do not show such an effect. Below about 200 MeV, the present psectrum also falls below the 1972 spectrum of Webber et al.(1973), but agrees reasonably well with the OGO-5 results of Fulks and Meyer (1973) between 50 and 200 MeV.

Figure 6 compares our positron results with those of earlier experiments. Here again there appears to be some discrepancy with our earlier results at about 150 MeV. We note that all of the earlier results, including those of Daugherty et al. (1975), used less detailed, and therefore presumably less accurate, models for the atmospheric electron production and propagation. For this reason, we feel that the results of Beuermann et al. (1970), should be considered as upper limits to the fluxes between 10 and 50 MeV. In any case, their results are consistent with our upper limits, despite having been measured at a time approaching the last solar maximum.

We now consider the implications of these results for the problem of solar modulation. The first requirement is a theoretical formulation describing the process of solar modulation. The modulation of galactic cosmic rays in the interplanetary medium has been discussed in terms of a spherically symmetry solar cavity within which the particles undergo convection, diffusion, and energy changes as a result of interactions with the expanding solar wind and associated magnetic fields. In such a model,

the particle number density is determined, in principle, by a Fokker-Planck equation where the solar wind speed, the diffusion coefficient, and interstellar particle spectrum are specified (e.g., Parker, 1965, 1966; Gleeson and Axford, 1967, 1968 a, b). The integration of the Fokker-Planck equation has been achieved for this analysis through a numerical technique due to Fisk (1971). A trial-and-error method was utilized to obtain the modulated spectra for comparison with our measurements. The solar wind speed was fixed at 400 km/sec and the radial distance to the boundary of the modulating region was taken as 10 AU. The radial dependence of the diffusion coefficient, K, was fixed; thus the parametric adjustments to find modulated spectra that fit the measurements involved varying the rigidity dependence and multiplicative constant of the diffusion coefficient. Since the total modulation depends principally on the integral of the diffusion coefficient over the volume of the modulating region, the selection of radial dependence and distance to the boundary are reasonably arbitrary, and affect only the multiplicative constant. The interstellar positron and total electron spectra are imposed as boundary conditions in order to solve for the modulated spectra.

The interstellar positron spectrum from Ramaty (1974)was used. In the 15 to 800 MeV energy interval, the positrons result principally from collisions of high energy cosmic rays with the interstellar medium. As the high energy cosmic rays are not greatly affected by solar modulation, their spectra can be accurately determined from measurements at earth. Thus, the greatest uncertainty in the calculation of the interstellar positron spectrum, in the energy region of interest, is the assumed

average cosmic ray path length, which Ramaty takes as 5 g $cm^{-2}$.

The interstellar electron spectrum is obtained from an analysis by Cummings et al. (1973), of measurements of the non-thermal radio spectrum in the direction of the galactic anti-center. The uncertainty is estimated by Cummings et al., to be a factor of 4 for electron energies above 300 MeV due mainly to uncertainties in the galactic magnetic field strength and the total line of sight emission length. The uncertainty in the electron spectrum increases toward lower energies, exceeding a factor of 50 near 100 MeV, primarily due to uncertainties in galactic parameters affecting interstellar radio absorption.

The positron data are able to most directly address the question of solar modulation in this energy region for two reasons: First, the calculated positron spectrum is accurately determined as discussed above. Second, the positrons in the 20 to 800 MeV energy range measured at 1 AU are very probably modulated galactic particles and not of solar or planetary origin.

Initial efforts to fit the positron data with a modulated spectrum yielded the best fit with a diffusion coefficient proportion to rigidity squared. Such a strong rigidity dependence, however, is in apparent disagreement with the rigidity dependence as deduced from the locally measured magnetic field power spectra (e.g., Jokipii, 1966).

Further efforts to improve the fit of the modulated positron spectrum to the measurements included exercising a solar modulation model due to Fisk (1975) which utilized off-ecliptic effects. The modulated spectrum could then be made to fall more steeply toward lower energies while maintaining a diffusion coefficient proportional to

rigidity by invoking a latitude dependent diffusion coefficient and solar wind speed. "Reasonable" choices of latitude dependence, however, did not result in a dramatic improvement of the fit of the modulated spectrum to the positron data, over the fit obtained with the spherically summetric model. The spherically symmetric model was then used with the constraint that the calculated modulated spectra would provide the best mutual fit to both the positron and total electron measurements. The results are shown in Figure 7. The interstellar positron spectrum has been raised by a factor of 2 which would correspond to an interstellar path length for the cosmic rays of about 10 g $cm^{-2}$. With this adjustment to the positrons, the positron and total electron modulated spectra are seen to be reasonably well fit by the measurements above 180 MeV by a model using a diffusion coefficient proportional to rigidity, as shown by the solid curve in Figure 7.

At energies below 180 MeV, two approaches are examined. The diffusion coefficient is first allowed to retain the same rigidity proportional form toward lower energy. This yields a modulated positron spectrum consistent with the upper limits in the low energy positron data; however, the total electron measurements are well above the resulting modulated total electron spectrum. These electrons must then be accounted for by a local source. A possible candidate is the Jovian magnetosphere, as suggested by Teegarden et al. (1974), to explain lower energy quiet time electron increases. The spectral index of 1.5 for electrons below 10 MeV, observed by Teegarden et al., in interplanetary electron increases, is consistent with the spectral index of the electron excess in our observations. In fact, the two balloon

flights which produced the data under discussion in this paper occurred just on either side of a large electron increase as observed by the IMP-7 low energy electron telescope.

Historically, in the absence of a viable local source for negatrons and less accurate galactic positron measurements, the diffusion coefficient was postulated to change its rigidity dependence. This results in a low energy modulated spectrum as indicated in Figure 7 by the dashed line. On the basis of the present data, this possibility cannot be excluded. Note that if the transition from a diffusion coefficient proportional to rigidity, to a constant value, were made in a less abrupt manner, the "valley" at about 180 MeV would diminish. This would improve the fit to the total electron spectrum but would have problems with the 95% confidence upper limit in the positron data at 150 MeV.

A more complete understanding of the interplanetary (and galactic) positron spectra await progress on several fronts. The critical parameters in solar modulation theory have yet to be directly measured out of the ecliptic plane, or at radial distances near the boundary region. In addition the plausibility of Jovian electrons with the required fluxes above 10 MeV remains unclear. Positron and negatron measurements in the 10 MeV to 1 GeV energy interval without the encumbrance of atmospheric secondaries could eliminate the ambiguity of interpretation still possible in this region.

## FIGURE CAPTIONS

Figure 1 - A schematic view of the instrument.

Figure 2 - Total electron fluxes from both flights for final portion of ascent and entire float period.

Figure 3 - Positron and negatron ascent data for representative energy intervals, from both flights combined.

Figure 4 - Positron and negatron spectra obtained from this experiment.

Figure 5 - Comparison of total electron spectra observed during the current solar minimum.

Figure 6 - Comparison of measured positron spectra between 10 and 2000 MeV.

Figure 7 - Modulation of interstellar spectra of positrons and total electrons. Solid line marked "modulated" shows effect of a diffusion coefficient proportional to rigidity. Dashed curve indicates the effect of setting the diffusion coefficient to a constant value below 180 MeV. Positron and negatron data points are from this experiment.

## REFERENCES


Beuermann, K.P., Rice, C.J., Stone, E.C , and Vogt, R.E. 1970, Acta Physica Academiae Scientiarum Hungaricae 29, Suppl. 1, 173.

Cummings, A.C., Stone, E.C., and Vogt, R.E. 1973, Proc. 13th Int. Conf. on Cosmic Rays, Denver, Colorado 1, 340.

Daniel, R.R. and Stephens, S.A. 1974, Reviews of Geophysics and Space Physics 12, 233.

Daugherty, J.K. 1974, NASA/GSFC Document X-660-74-16 (unpublished).

Daugherty, J.K., Hartman, R.C., and Schmidt, P.J. 1975, Ap. J. 197, in press.

Fanselow, J.L., Hartman, R.C., Hildebrand, R.H., and Meyer, P. 1969, Ap. J. 158, 771.

Fisk, L.A. 1975, Private Communication.

Fisk, L.A. 1971, Journal of Geophysical Research 76, 221.

Fulks, G., Meyer, P., and L'Heureux, J. 1973, Proc. 13th Int. Conf. on Cosmic Rays, Denver, Colorado 2, 753.

Gleeson, L.J., and Axford, W.I. 1967, Ap. J. 149, L115

Gleeson, L.J., and Axford, W.I. 1968a, Can. J. Physics 46, 937.

Gleeson, L.J., and Axford, W.I. 1968b, Ap. J. 154, 1011.

Goldstein, M.L., Ramaty, R., and Fisk, L.A. 1970, Phys. Rev. Letters 24, 1193.

Israel, M.H., and Vogt, R. 1969, J. Geophys. Res. 74,1974.

Jokipii, J.R., L'Heureux, J., and Meyer, P. 1968, J. Geophys, Res. 73, 1593.

Jokipii, J.R. 1966, Ap. J. 146, 480.

Parker, E.N. 1965, Planet. Space Sci. 13, 9.

Parker, E.N. 1966, Planet. Space Sci. 14, 371.

Ramaty, R. 1974, Cosmic Electrons, High Energy Particles and Quanta in Astrophysics, ed. F.B. McDonald and C.E. Fichtel, MIT Press, Cambridge, Mass.

Teegarden, B.J., McDonald, F.B., Trainor, J.H., Webber, W.R.,and Roelof, E.C. 1974, NASA/GSFC Document X-660-74-197.

Webber, W.R. 1968, J. Geophys. Res. 73, 4909.

Webber, W.R., Kish, J., and Rockstroh, J.M. 1973, Proc. 13th Int. Conf. Cosmic Rays, Denver, Colorado 2, 760.

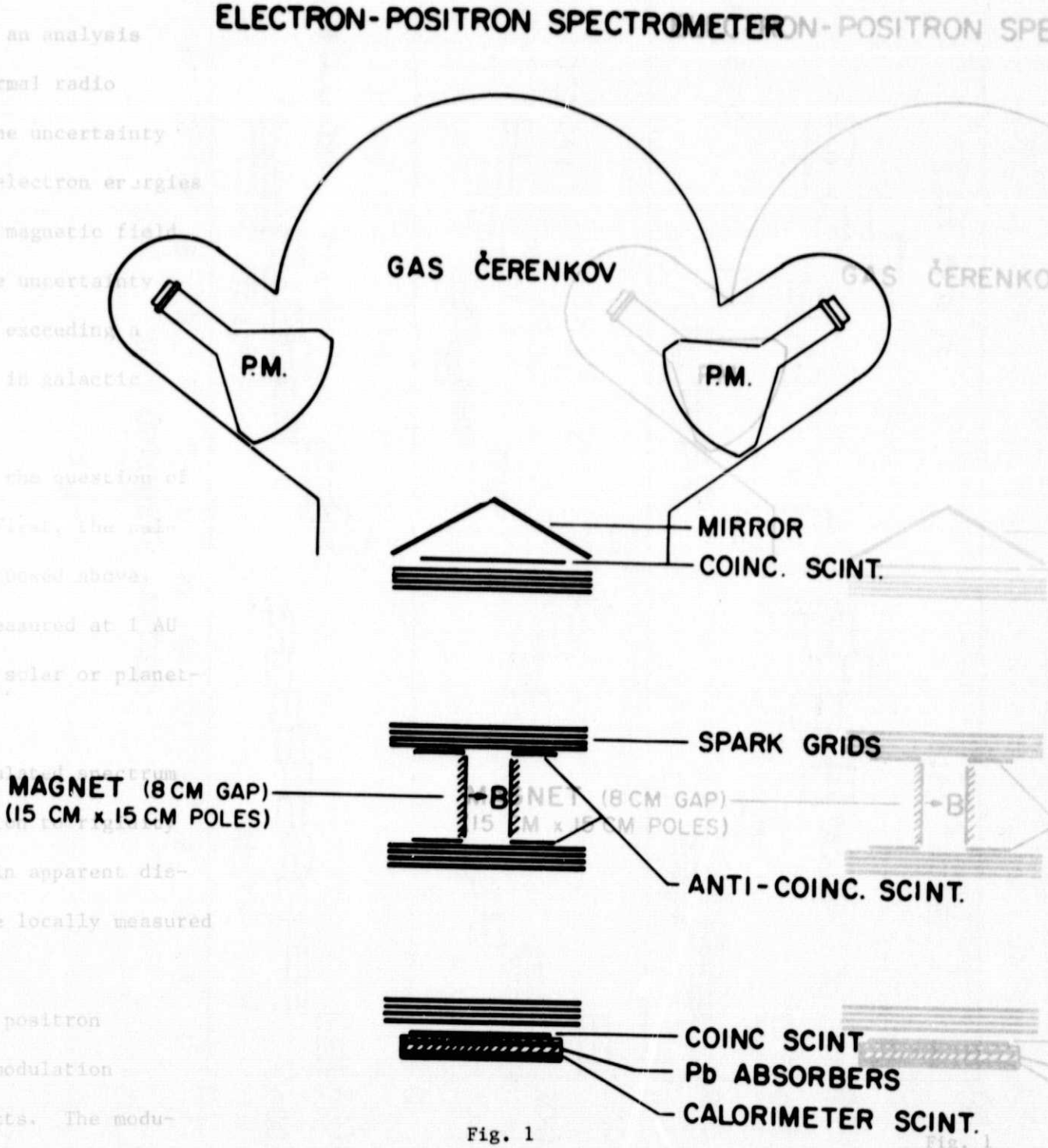


Fig. 1

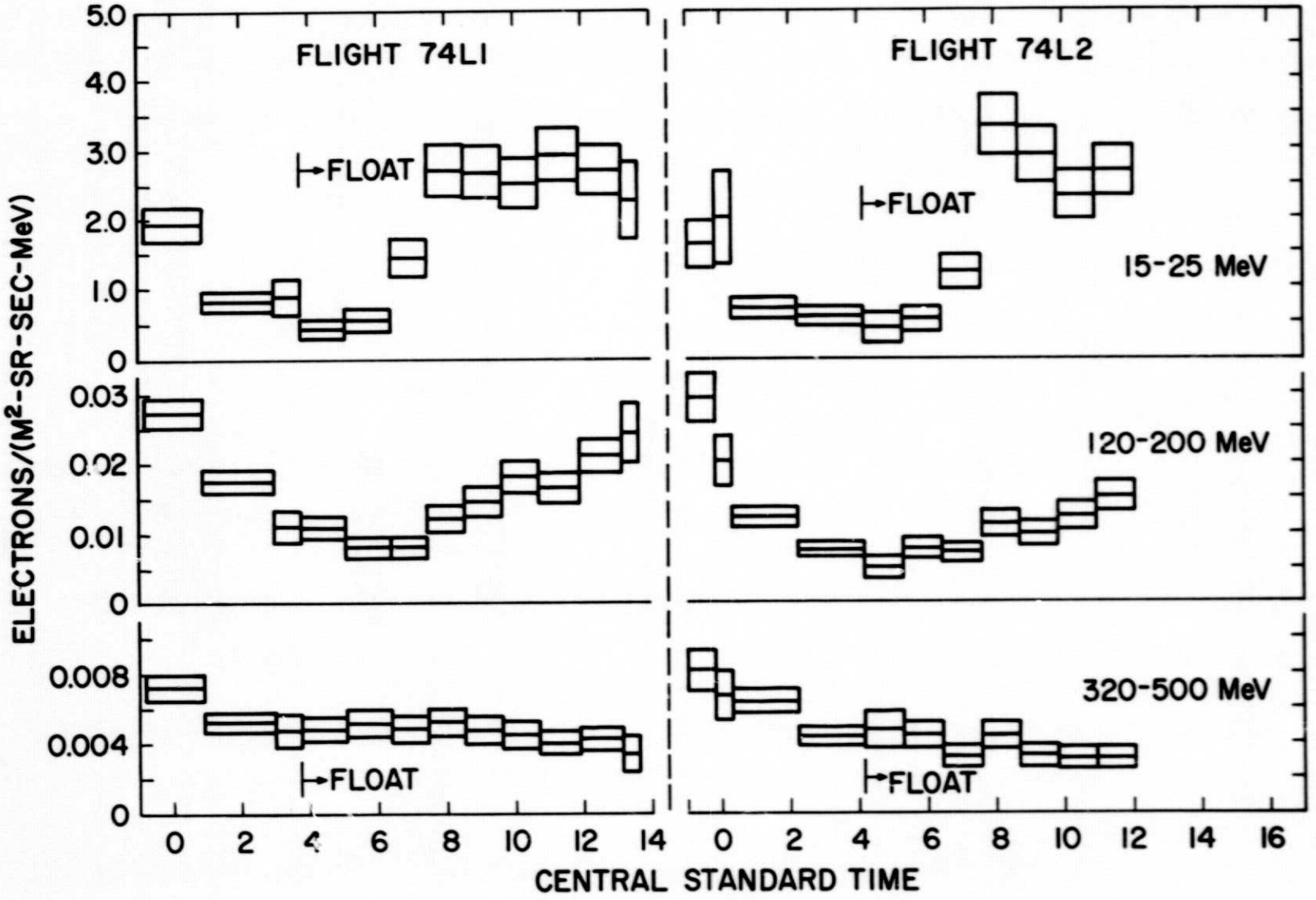
FLIGHT 74L1
FLIGHT 74L2
FLOAT
FLOAT
FLOAT
FLOAT
15-25 MeV
120-200 MeV
320-500 MeV
ELECTRONS/(M²-SR-SEC-MeV)
5.0
4.0
3.0
2.0
1.0
0
0.03
0.02
0.01
0
0.008
0.004
0
0 2 4 6 8 10 12 14
0 2 4 6 8 10 12 14 16
CENTRAL STANDARD TIME

Fig. 2

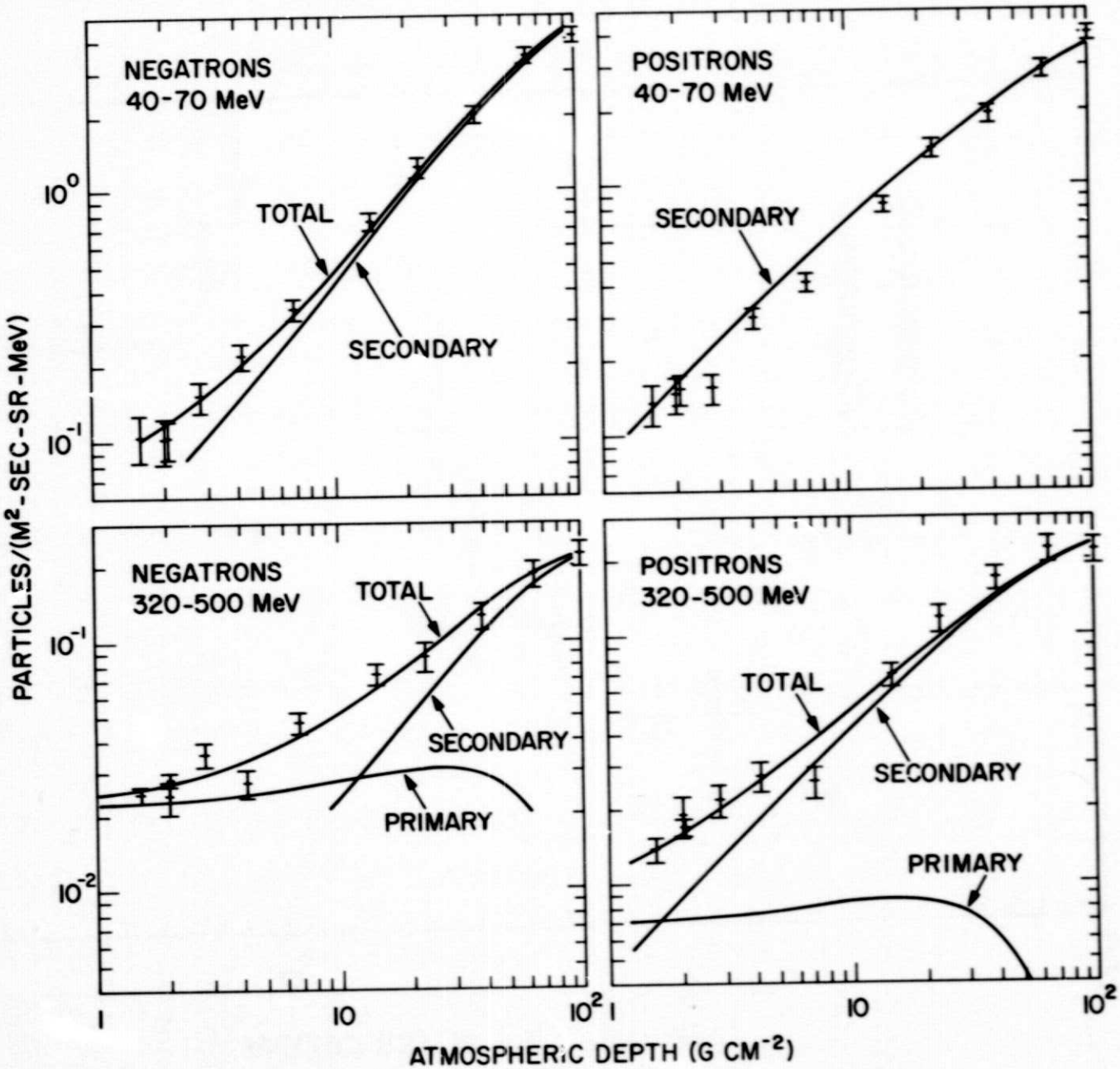
NEGATRONS
40-70 MeV
TOTAL
SECONDARY
POSITRONS
40-70 MeV
SECONDARY
NEGATRONS
320-500 MeV
TOTAL
SECONDARY
PRIMARY
POSITRONS
320-500 MeV
TOTAL
SECONDARY
PRIMARY
PARTICLES/(M²-SEC-SR-MeV)
ATMOSPHERIC DEPTH (G CM⁻²)
10⁰
10⁻¹
10⁻²
1
10
10²

Fig. 3

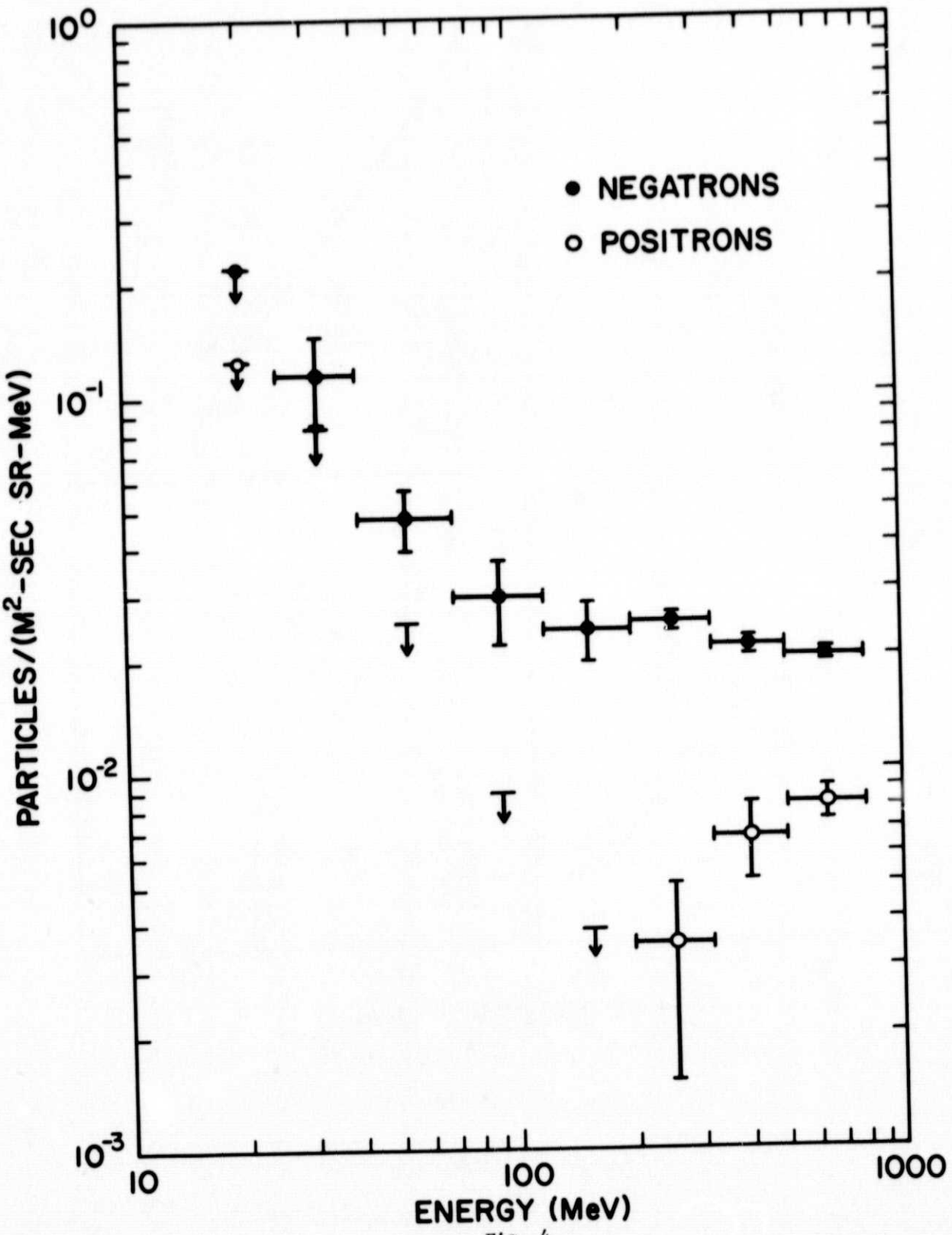
NEGATRONS
POSITRONS
PARTICLES/(M²-SEC SR-MeV)
10⁰
10⁻¹
10⁻²
10⁻³
10
100
1000
ENERGY (MeV)

Fig. 4

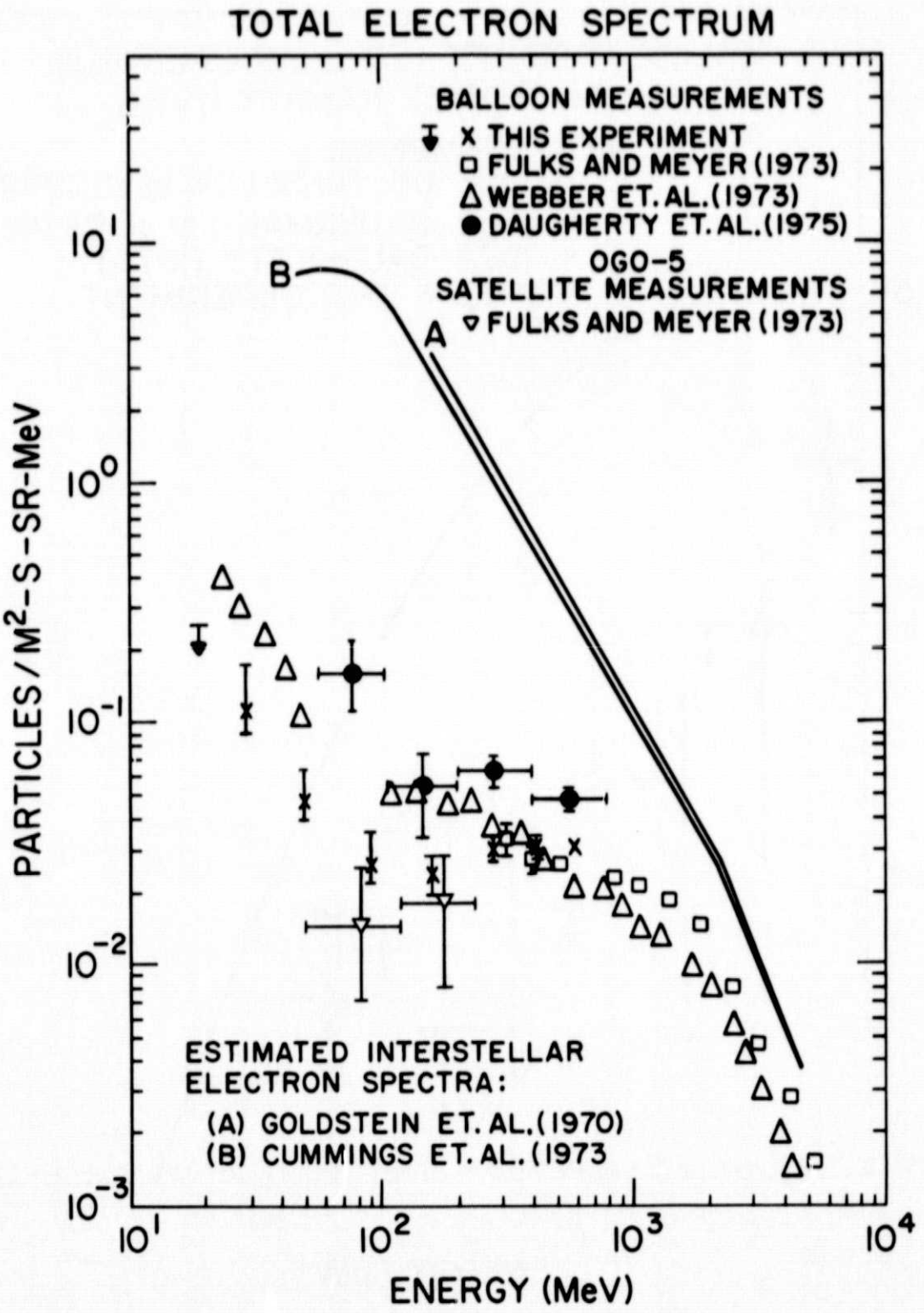
TOTAL ELECTRON SPECTRUM
BALLOON MEASUREMENTS
X THIS EXPERIMENT
FULKS AND MEYER (1973)
WEBBER ET. AL. (1973)
DAUGHERTY ET. AL. (1975)
OGO-5
SATELLITE MEASUREMENTS
FULKS AND MEYER (1973)
B
A
ESTIMATED INTERSTELLAR
ELECTRON SPECTRA:
(A) GOLDSTEIN ET. AL. (1970)
(B) CUMMINGS ET. AL. (1973
PARTICLES / M2-S-SR-MeV
ENERGY (MeV)
10^1
10^0
10^-1
10^-2
10^-3
10^1
10^2
10^3
10^4

Fig. 5

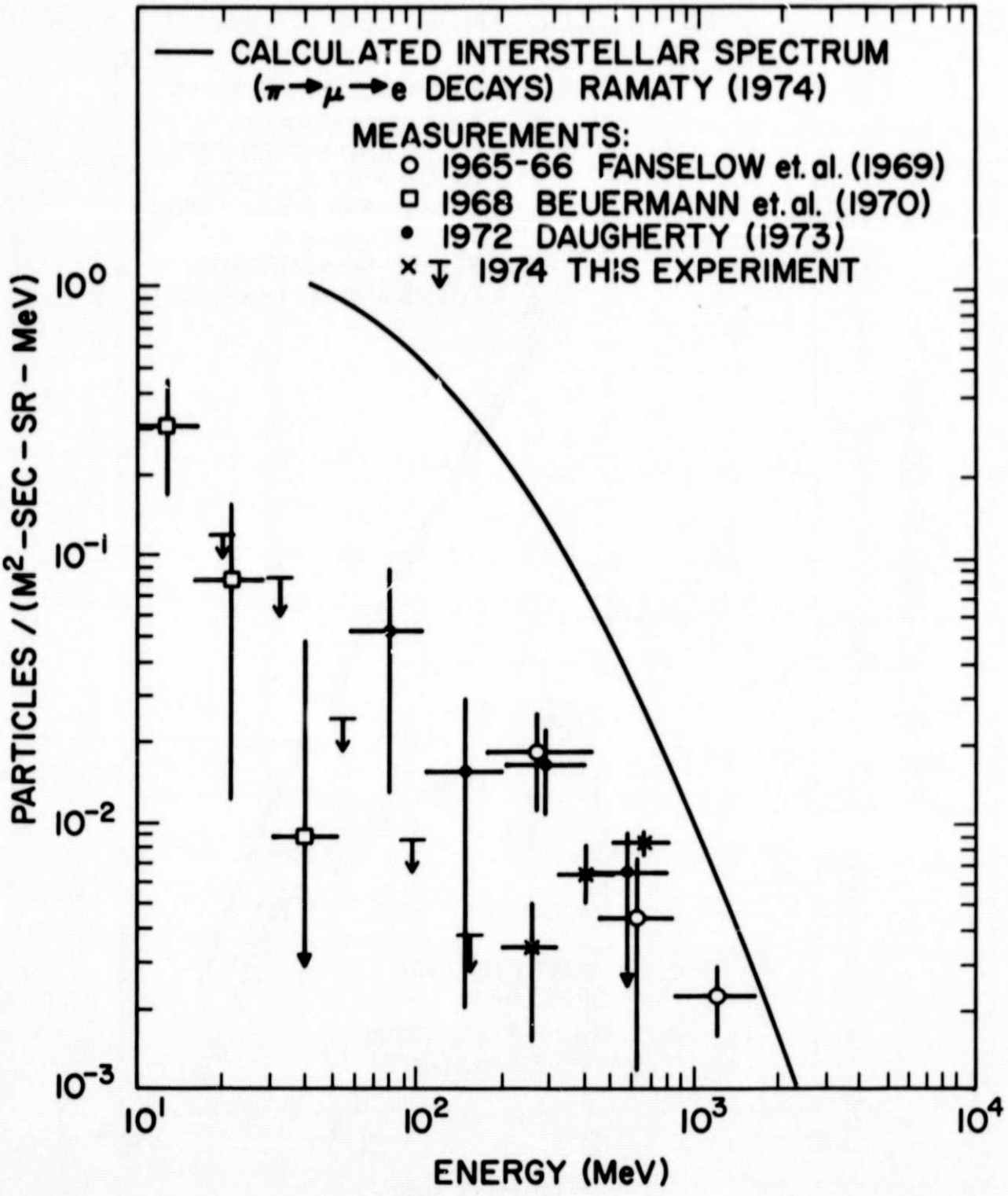
CALCULATED INTERSTELLAR SPECTRUM
(π→μ→e DECAYS) RAMATY (1974)
MEASUREMENTS:
1965-66 FANSELOW et. al. (1969)
1968 BEUERMANN et. al. (1970)
1972 DAUGHERTY (1973)
1974 THIS EXPERIMENT
PARTICLES / (M²-SEC-SR-MeV)
10⁰
10⁻¹
10⁻²
10⁻³
10¹
10²
10³
10⁴
ENERGY (MeV)

Fig. 6

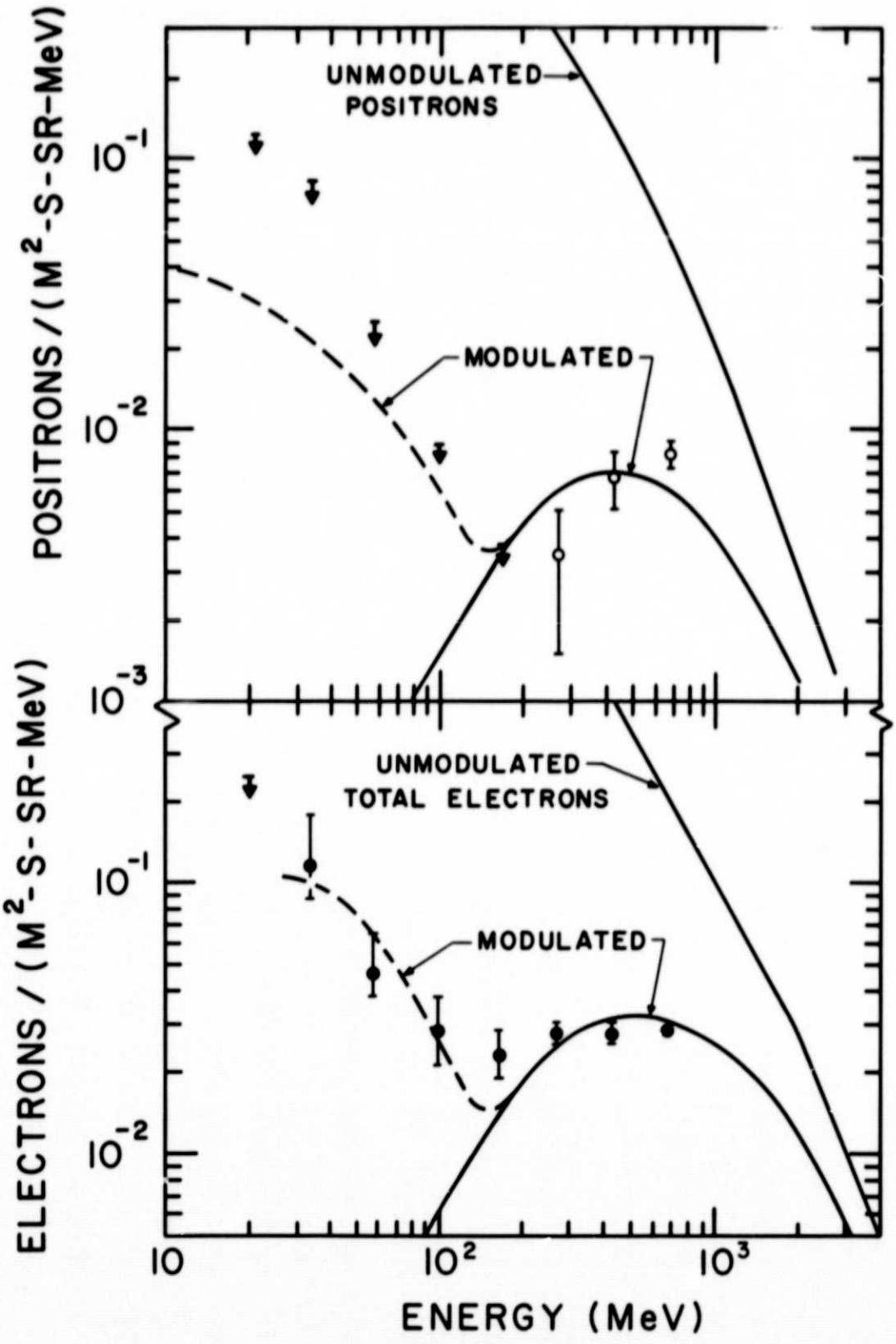
UNMODULATED
POSITRONS
MODULATED
POSITRONS / (M²-S-SR-MeV)
10⁻¹
10⁻²
10⁻³
UNMODULATED
TOTAL ELECTRONS
MODULATED
ELECTRONS / (M²-S-SR-MeV)
10⁻¹
10⁻²
10
10²
10³
ENERGY (MeV)

Fig. 7